An exploratory study of phosphorus release from biomass by carbothermic reduction reactions

N.B. When citing this work, cite the original published paper.

(article starts on next page)

An exploratory study of phosphorus release from biomass by carbothermic reduction reactions

Emil O. Lidman Olsson [a,b,c], Peter Glarborg [a], Henrik Leion [d], Kim Dam-Johansen [a], Hao Wu [a,*]

[a] *Department of Chemical and Biochemical Engineering, Technical University of Denmark, Søltofts Plads, Building 229, 2800 Kgs. Lyngby, Denmark*
[b] *Sino-Danish College, University of Chinese Academy of Sciences, Eastern Yanqihu campus, 380 Huaibeizhuang, Huairou district, Beijing, 101400, China*
[c] *Sino-Danish Center for Education and Research, Eastern Yanqihu campus, 380 Huaibeizhuang, Huairou district, Beijing, 101400, China*
[d] *Department of Chemistry and Chemical Engineering, Chalmers University of Technology, Kemigården 4, 412 96 Gothenburg, Sweden*

Abstract

Phosphorus (P) from biomass can cause operational problems in thermal conversion processes. In order to explore the release mechanism of P to the gas phase, carbothermic reduction of meta-, pyro-, and orthophosphates of ash elements commonly found in biomass; sodium, potassium, magnesium, and calcium was investigated. Mixtures of each phosphate and activated carbon were heated to 1135 °C in a laboratory-scale reactor, with the CO and CO_2 evolving from the sample monitored, and the chemical composition of selected residues analyzed to quantify the release of P. Thermal gravimetric analysis was also performed on selected samples. The alkaline earth phosphates were reduced in steps, following the sequence meta → pyro → ortho → alkaline earth oxide. However, the alkali metaphosphates appear to be reduced in one step, in which both alkali and P are released. Alkali pyro- and orthophosphate appear to undergo a two-step process. In the first step, mainly alkali is released and in the second step both alkali and P. An intermediate is produced in the first step, which has a K:P:O atomic ratio of about 2:1:2.7, indicating it might be a phosphite with the overall stoichiometry; $K_4P_2O_5$. The reduction of alkaline earth phosphates could be interpreted using available thermodynamic data, whereas thermodynamic equilibrium calculations for the alkali phosphates did not correspond well to the experimental observations. Kinetics were derived for the different reduction reactions, and can be used to compare the reactivity of the phosphates. The work suggests that carbothermic reduction reactions are important for the release of P in the temperature range 850–1135 °C and relevant for biomass combustion, pyrolysis and gasification.

---

* Corresponding author.
 E-mail address: haw@kt.dtu.dk (H. Wu).

Introduction

Biomass residues from agriculture and process industries can be used in thermal conversion processes to produce heat, power, gas/liquid fuels, or chemicals. However, using these fuels can be challenging because of their complex ash composition. One of the ash-forming elements that can be problematic is Phosphorus (P). Examples of P-rich biomass include seed- and grain-originated biomass, such as wheat bran/grain from bioethanol production [1], rapeseed meal from biodiesel production [2], or animal biomass such as litter [3], manure [4], and meat and bone meal [5]. Some of these biomasses have been reported to cause problems in thermal conversion processes such as bed agglomeration in fluidized bed combustion [6], deposit formation in economizers and clogging of filter units in grate combustion [1], and deactivation of SCR catalysts in pulverized fuel combustion [7]. Several of these problems are related to the release of P species to the gas phase. The release of P was investigated only for a few biomasses [1,8–10] and the responsible mechanism(s) has not been experimentally verified.

Most of the P in grain- and seed-originated biomass is present in the form of the organic molecule phytate. Recently it was shown that upon heating, sodium phytate decomposes into inorganic Na-phosphate and a char structure [11]. Above 800 °C, the Na-phosphate reacts with the char in a carbothermic reduction reaction, resulting in the formation of gaseous elemental P and CO. Whether similar reactions take place for other phosphates expected to be present in biomass, such as K-, Mg-, and Ca-phosphates, at temperatures relevant for combustion, pyrolysis and gasification of biomass has not been thoroughly investigated. Carbothermic reduction of phosphates, especially Ca-phosphate in phosphate rock, has long been used to produce elemental P and H_3PO_4 industrially [12,13]. Despite its importance, the detailed reaction mechanism seems not to be fully understood. For Na, K, and Mg, only the ultraphosphates ($M_2O/P_2O_5<1$) [14], a mixed Na-K-Mg ultraphosphate [15], and the alkali metaphosphates [16] were investigated, using a C/P molar ratio of 5 and mainly at temperatures greater than 1000 °C. In biomass and biomass char, the C/P molar ratio is significantly higher and temperatures below 1000 °C are also of interest for thermal conversion processes.

In this work, the reduction of meta-, pyro- and orthophosphates of Na, K, Mg and Ca are investigated systematically in a temperature range relevant for combustion, pyrolysis and gasification of biomass in fixed bed and fluidized bed reactors. The kinetics of the reactions are determined by analysis of the CO and CO_2 evolution in the off-gas and using thermal gravimetric analysis (TGA). Thermodynamic equilibrium calculations are used to in-vestigate if the observed reactions can be described with available thermodynamic data.

Materials and methods

Materials

The following phosphates were supplied by Merck; $NaH_2PO_4 \cdot H_2O$ (>99%, product no. 6346), Na_2HPO_4 (>98%, S-7907), Na_3PO_4 (96%, 342483), KH_2PO_4 (≥99%, P0662), K_2HPO_4 (≥98%, P3786), K_3PO_4 (≥98%, P5629), $Ca(H_2PO_4)_2$ (≥95%, C8017), and $Ca_3(PO_4)_2$ (≥96%, 21218). $Mg_2P_2O_7$ (≥98%, 39317) and $Ca_2P_2O_7$ (96%, 89836) were supplied by Alfa Aesar. $Mg_3(PO_4)_2$ (≥98%, 39194) was supplied by Acros Organics as a hydrate with an unspecified content of water and was therefore dried at 800 °C for 1 h prior to use. $Mg(PO_3)_2$ was synthesized from $Mg_2P_2O_7$ and H_3PO_4(aq). The details are available in the Supplementary Material (SM). The H_3PO_4 was supplied by Fluka (product no. 79623). Activated carbon, sold as a filter material for beverage purification, was purchased in retail.

The activated carbon was mixed with phosphates in a C/P molar ratio of 25/1 resulting in a 10-fold excess of C as per the overall reaction (expressed on the basis of one released phosphorus atom):

$$\tfrac{1}{2}P_2O_5(s) + \tfrac{5}{2}C(s) \rightarrow \tfrac{1}{4}P_4(g) + \tfrac{5}{2}CO(g) \qquad \text{(R1)}$$
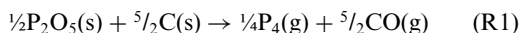
The large excess of C limits the interaction between the phosphate and the sample crucible, and enables approximating the reaction as first-order in phosphate concentration only. The used C/P molar ratio is representative for biomass and biomass char, which have molar ratios in the same order of magnitude. The carbon and phosphate were mixed and milled to a fine powder in a cryogenic mill.

The hydrated phosphates are known to decompose in the temperature ranges specified in Table 1, which are much lower than the temperatures required by the carbothermic reduction. All H is therefore assumed to have left the sample prior to the carbothermic reduction reaction takes place.

Experiments in horizontal tube reactor and sample characterization

A sample mass of 2.8–3.7 g (depending on the phosphate, but corresponding to 7.2 mmol P in each sample) was placed in an alumina crucible and heated in a horizontal tube reactor described previously [11]. A gas flow of 3 L/min (20 °C, 1 atm) of N_2 was fed to the reactor while the temperature was increased from 25 to 1135 °C at a maximum rate of 15 °C/min. The temperature profile is nonlinear due to significant heat losses at higher temperatures. When the final temperature was reached,

Table 1
Decomposition of hydrated phosphates.

Phosphate			Temperature (°C)
$NaH_2PO_4 \cdot H_2O$	$\rightarrow$	$NaPO_3 + 2H_2O$	<190 [17]
Na_2HPO_4	$\rightarrow$	$\frac{1}{2}Na_4P_2O_7 + \frac{1}{2}H_2O$	215–280 [18]
KH_2PO_4	$\rightarrow$	$KPO_3 + H_2O$	200–340 [18]
K_2HPO_4	$\rightarrow$	$\frac{1}{2}K_4P_2O_7 + \frac{1}{2}H_2O$	282–400 [19]
$Ca(H_2PO_4)_2$	$\rightarrow$	$Ca(PO_3)_2 + 2H_2O$	280 [20]

the sample was cooled quickly. The CO and CO_2 concentration in the off-gas was measured using an analyzer from Emerson Process Management, of type Rosemount MLT4, with infrared sensors.

The kinetics of the carbothermic reduction reaction was determined assuming a first-order reaction according to:

$$\frac{dn_P}{dt} = -k_0 e^{-\frac{E_a}{RT}} \cdot n_P \qquad (1)$$

where n_P (mol) is the amount of phosphate remaining in the sample, t (s) is the time, k_0 (s^{-1}) is the pre-exponential factor, E_a ($J \cdot mol^{-1}$) is the activation energy, R ($J \cdot K^{-1} \cdot mol^{-1}$) is the universal gas constant, and T (K) is the temperature. The change in amount of phosphate was taken as the evolution of $CO + CO_2$ according to the equation:

$$\frac{dn_P}{dt} = -x\dot{n}_C \qquad (2)$$

where $\dot{n}_C$ (mol/s) is the molar flow of $CO + CO_2$, calculated using the CO and CO_2 gas analysis and the ideal gas law, and x the number of $CO + CO_2$ evolving per phosphate reacting. x depends on the stoichiometry of the carbothermic reduction reaction, which is known for some phosphates, and was determined using the weight loss and chemical composition of residues for other phosphates. Values used for x are available in Table S4 in the SM. n_P was calculated by integration of Eq. (2). k_0 and E_a were found using linear regression. A good linear fit could only be obtained for the first part of the reaction. This might be a consequence of factors such as: 1) the formed product reacting further, 2) mass transfer limitations between the carbon and the phosphate particle boundary, as well as within the phosphate particle, 3) the accuracy of the $CO + CO_2$ quantification, and 4) the assumption of a first-order reaction in P content.

In the experiments, CO_2 accounted for only about 5% at most of the evolved CO and CO_2. The presence of CO_2 might be caused by CO also acting as a reducing agent in the reaction, oxidation of CO by small amounts of oxygen present in the system, or by side reactions taking place. Therefore, it can be debated how CO_2 should be accounted for in Eq. (2), but for simplicity, and considering the rather low amounts, it was decided to treat it as equivalent to CO.

The delay in measured CO and CO_2 concentrations, caused by equipment residence time as well as

analyzer response time, and the dispersion of CO and CO_2 in the off-gas path were accounted for by deconvolution of the experimental data using the result from a step-change test (details are available in SM).

The weight loss of each sample was calculated using the weight of the empty crucible, the weight of the sample prior to the experiment, and the weight of the crucible containing the sample residue after the experiment.

Selected experimental runs were repeated and showed that the weight loss and $CO + CO_2$ profile could be satisfactorily reproduced.

A run using carbon only was performed to determine the weight loss and $CO + CO_2$ release from the carbon itself. The data were used to correct the other runs and are shown in the SM.

The elemental composition of selected sample residues was quantified using inductively coupled plasma with optical emission spectrometry (ICP-OES). Digestion was performed according to United States Environmental Protection Agency (US EPA) method 3052. The samples were analyzed in duplicates.

Thermal gravimetric analysis (TGA)

TGA was performed on selected samples to verify that the weight loss corresponded to the measured $CO + CO_2$ and reaction stoichiometry. An analyzer from Netzsch, of type STA 449 F1 Jupiter ASC was used. Around 5 mg of sample was loaded in an Al_2O_3 crucible and heated to 1135 °C in 200 mL/min N_2 at a heating rate of 10 °C/min.

The kinetic parameters of the reactions were calculated similarly to above, but dn_P/dt and n_P were here derived using the weight measurement according to:

$$\frac{dn_P}{dt} = \frac{dm}{dt}\left(\frac{1}{xM_{CO} + yM_P + zM_M}\right) \qquad (3)$$

where m (g) is the mass of the sample, and M_{CO} (g/mol), M_P (g/mol), and M_M (g/mol) is the molar mass of CO, P and alkali respectively, and y and z are the number of P and alkali atoms leaving the sample per phosphate reacting respectively. y and z are determined in the same manner as described for x above. Values used for x, y, and z are available in Table S4 in the SM.
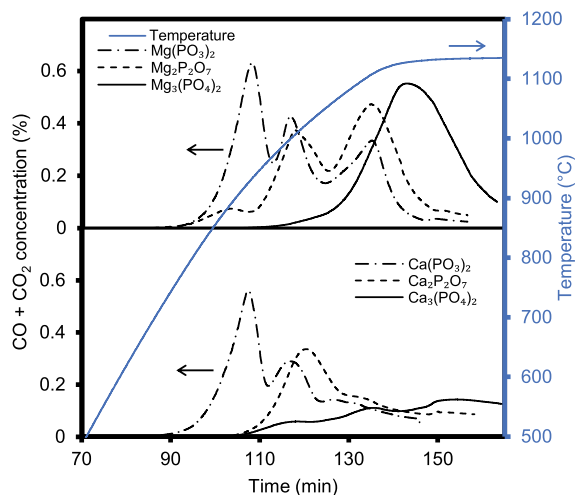
Fig 1. CO+CO_2 concentration measured in off-gas (left axis) and temperature (right axis) during carbothermic reduction of Mg- (upper) and Ca- (lower) phosphates.

Thermodynamic equilibrium calculations

To understand if the observed reactions can be described with available thermodynamic data, thermodynamic equilibrium calculations were performed using the commercially available software FactSage, version 7.3 [21]. The FactPS database (solids and gas species) was used, together with the FToxid database (solids and solution model SLAGA) for the alkaline earth phosphate systems, and the data from [22] (solids and non-ideal solution model) for the alkali phosphate systems because it contains transparent modeling details for the non-ideal molten solutions. The thermodynamic data for PO_2, P_4O_6 and $NaPO_3$ used in [11] were adapted. Thermodynamic data for $KPO_3(g)$ were calculated and included in the model (details in the SM). A list of all species included in the model is provided in the SM.

The same molar compositions as in the physical samples were used in the modeling, and a N_2 content corresponding to 10 min of the gas flow in the horizontal tube reactor was applied.
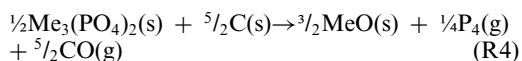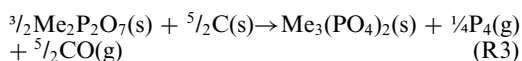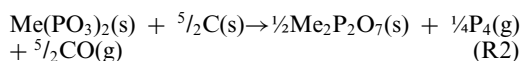
Results and discussion

Alkaline earth (Mg, Ca) phosphates

The CO+CO_2 concentration in the gas passed over the Mg- and Ca-phosphates mixed with carbon can be seen in Fig. 1. For the metaphosphates, two distinct peaks appear in the same temperature range (approx. 850–950 °C). A clear third peak is present for the Mg-metaphosphate, whereas it is less distinct for the Ca-phosphate. Similarly, the pyrophosphates both have a peak in the same tem-

perature range (approx. 950–1050 °C), followed by a second peak for the Mg-pyrophosphate, and a tail-like profile for the Ca-pyrophosphate. For the Mg-orthophosphate, one large peak is apparent at higher temperatures (approx. 1100–1135 °C), whereas the reaction seem to be much slower for the Ca-orthophosphate.

In the literature, carbothermic reduction reactions of $Ca_3(PO_4)_2$ have been studied extensively because of the relevance for P production from phosphate rock [12,13]. It was previously shown that Ca- [23] and Mg-phosphates [14,15] are reduced in a stepwise manner following the overall reactions below, expressed on the basis of one released phosphorus atom (Me = Ca or Mg):

$$Me(PO_3)_2(s) + {}^5/_2C(s) \rightarrow {}^1/_2Me_2P_2O_7(s) + {}^1/_4P_4(g) + {}^5/_2CO(g) \qquad (R2)$$

$$^3/_2Me_2P_2O_7(s) + {}^5/_2C(s) \rightarrow Me_3(PO_4)_2(s) + {}^1/_4P_4(g) + {}^5/_2CO(g) \qquad (R3)$$

$$^1/_2Me_3(PO_4)_2(s) + {}^5/_2C(s) \rightarrow {}^3/_2MeO(s) + {}^1/_4P_4(g) + {}^5/_2CO(g) \qquad (R4)$$

The above sequence; meta → pyro → ortho→ alkaline earth oxide, fits well with the observations in this work. R2 and R3 take place in a similar temperature range for Ca and Mg phosphates, whereas R4 appears to be faster for Mg, compared to Ca. The conversion of the phosphates, when assuming the process proceeds according to reactions R2-R4, is shown in Table 2. Generally, the conversion calculated based on mass loss fit well with the value calculated using the CO+CO_2 analysis. For the Mg-phosphates, the conversion appear to be almost complete, which is also the case judging by the

Table 2
Fraction of phosphate reacted (%), calculated based on mass loss and $CO+CO_2$ release for samples treated in the tube reactor.

	Phosphate	Mass loss	$CO+CO_2$ release
Mg[a]	$Mg(PO_3)_2$	84	90
	$Mg_2P_2O_7$	84	84
	$Mg_3(PO_4)_2$	78	89
Ca[a]	$Ca(PO_3)_2$	75	70
	$Ca_2P_2O_7$	48	53
	$Ca_3(PO_4)_2$	37	36
Na[b]	$NaPO_3$	87	106
	$Na_4P_2O_7$	84	89
	Na_3PO_4	87	86
K[b]	KPO_3	76	101
	$K_4P_2O_7$	81	106
	K_3PO_4	84	90

[a] For Mg- and Ca-phosphates, the calculation is based on the reaction proceeding according to R2-R4.
[b] For Na- and K-phosphates, the calculation is based on every O atom leaving as CO, and all alkali metal is released.

$CO+CO_2$ profile. For the Ca-phosphates, the profile indicates that the reactions were not completed by the end of the run. This is supported by the lower values in Table 2.

$CO+CO_2$ evolves from $Ca_3(PO_4)_2$ in two small peaks before it reach the final peak at around 150 min. These two peaks might be caused by the reduction to $Ca_{10}(PO_4)_6O$ and $Ca_4(PO_4)_2O$, which are located between $Ca_3(PO_4)_2$ and CaO in the $CaO-P_2O_5$ phase diagram [24]. The corresponding Mg-phosphates are not known to exist and might explain why $Mg_3(PO_4)_2$ exhibits only one large peak.

Alkali (Na, K) phosphates

Since only a few data on carbothermic reduction of alkali phosphates are available in the literature, especially for pyro- and orthophosphates, TGA analysis was performed for these samples. The results are shown in Fig. 2. The reactions take place in a similar temperature range for all phosphates (above approx. 900 °C). Based on the $CO+CO_2$ profile, it seems to be a two step process for the pyro- and orthophosphates, whereas only one peak is visible for the metaphosphates. It is not clear if the alkali phosphates are reduced in a stepwise manner analogously to the alkaline earth phosphates as in R2-R4. Interestingly, the TGA analysis reveals that most of the weight loss is associated with the second step, whereas most of the CO and CO_2 seem to be released in the first step.

In order to understand the two-step process taking place for the alkali pyro- and orthophosphates, a run using K_3PO_4 was repeated, but this time the sample was quickly cooled after the first $CO+CO_2$ peak (at 123 min into the run). The amounts of alkali and P in the intermediate sample collected after the first $CO+CO_2$ peak, and in the final product were quantified, as shown in Fig. 2. It is apparent that mainly K (46%) is released during the first part of the process, whereas only some of the P (17%) is released. The intermediate sample mixture had a bulk K/P molar ratio of 2.0. Based on the amount of $CO+CO_2$ leaving with the off-gas, the O/P molar ratio of the intermediate should be around 2.7. With these molar ratios, the intermediate should have an overall composition corresponding to a phosphite; $K_4P_2O_5$ (not to be confused with the pyrophosphate; $K_4P_2O_7$). There are no records of such a compound in the literature, which is not surprising considering that few studies on carbothermic reduction of alkali phosphates have been presented. However, phosphites have previously been suggested to act as intermediates in carbothermic reduction of calcium phosphate [25]. Previous thermal decomposition studies of the hypophosphites Na_2HPO_3 [26–28] and K_2HPO_3 [26] have shown that, after loss of H_2, the residues had an overall composition corresponding to $M_4P_2O_6$ (M = Na or K) and were stable to at least 700 °C [26]. The residues were reported to consist of elemental P (20% of P), $M_4P_2O_7$ (40%) and M_3PO_4 (40%) [27]. However, XRD analysis of the intermediate sample obtained in this work did not detect those phases, but did show one or more phases that could not be identified. The intermediate was also analyzed using ATR-FTIR. The spectrum did not have pronounced peaks in the range typical for phosphates (<1200 cm^{-1}), but instead had two pronounced peaks at higher wavenumbers (1200–1500 cm^{-1}) which might be associated with phosphite judging by the spectrum of Na phosphite (Na/P = 2) in [29]. The XRD and ATR-FTIR spectrum are available in the SM. Since the specific phases of the intermediate could not be identified, it will here be referred to as $M_4P_2O_5$. Detailed characterization may be subject to future work.

Based on the composition of the intermediate, the $CO+CO_2$ analysis, and the TGA result, the first step in the reduction of M_3PO_4 is proposed to be:

$$M_3PO_4(s) + {}^3/_2C(s) \rightarrow {}^1/_2M_4P_2O_5(s, l) + M(g) + {}^3/_2CO(g) \qquad (R5)$$
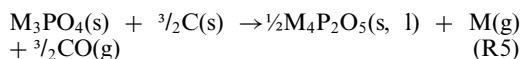
Based on the elemental composition of the final sample residues it is clear that most of the alkali and P were released from the sample. This is in agreement with the mass loss of the samples investigated in the tube reactor. The $CO+CO_2$ measurement also reveals that most of the oxygen was released. The conversion calculated based on mass loss or $CO+CO_2$ release, assuming the entire phosphate can be reduced and leave the sample, is shown in Table 2. Most of the oxygen in the sample seemingly reacted, and the mass loss and elemental composition show that only small amounts of alkali
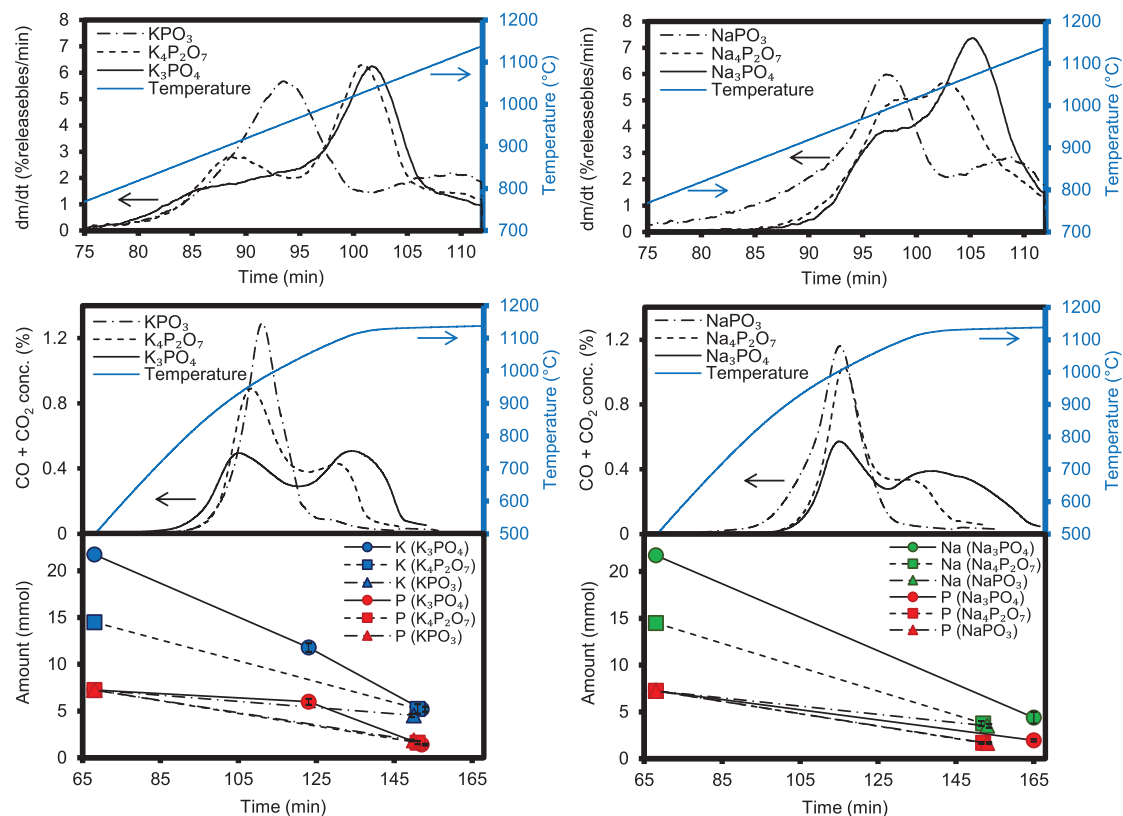
Fig 2. Mass loss rate determined using TGA (upper), $CO+CO_2$ concentration measured in off-gas from horizontal tube reactor (middle) together with amount of P and alkali in samples (lower) for K- (left) and Na- (right) phosphates. Data for lower temperatures are not shown because no CO or CO_2 is evolving, and the release of alkali and P is negligible. The mass loss rate is given as% releasables per min, where releasables represent the salt (MPO_3, $M_4P_2O_7$ or M_3PO_4) and the theoretical amount of carbon that can leave as CO. The bulk amount of P and alkali prior to reaction was calculated based on the amount of phosphate and carbon used to prepare the sample, whereas it for the final residue and K_3PO_4 intermediate was determined using ICP-OES. Error bars represent estimated expanded uncertainty for ICP-OES analysis.

and P was still present in the sample residues. Overall, the second step of the M_3PO_4 reduction may therefore be written as:

$$\tfrac{1}{2}M_4P_2O_5(s, l) + \tfrac{5}{2}C(s) \rightarrow \tfrac{1}{4}P_4(g) + 2M(g) + \tfrac{5}{2}CO(g) \quad (R6)$$
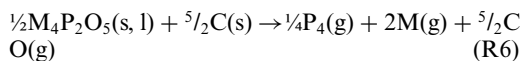
The process for the alkali pyrophosphates is not easily explained. The second reduction step take place in the same temperature range for both M_3PO_4 and $M_4P_2O_7$. The same intermediate may therefore be involved. A straightforward reduction could, overall, be written as:

$$M_4P_2O_7(s) + 2C(s) \rightarrow M_4P_2O_5(s, l) + 2CO(g) \quad (R7)$$

However, this would result in only 2/7 (29%) of the $CO+CO_2$ evolving in the first peak, which is not in agreement with the experimental observation where about 70% of the $CO+CO_2$, for both $K_4P_2O_7$ and $Na_4P_2O_7$, is found in the first peak. Additionally, the TGA data indicates a greater mass loss. It is known that $M_4P_2O_7$ thermally decompose and vaporize by forming $M_3PO_4(s)$ and $MPO_3(g)$ [12]. A similar process may take place in this case, where the MPO_3 unit undergoes further reduction:

$$M_4P_2O_7(s) + 3C(s) \rightarrow M_3PO_4(s) + M(g) + \tfrac{1}{4}P_4(g) + 3CO(g) \quad (R8)$$
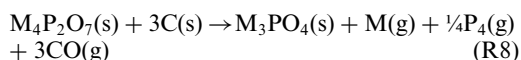
The formed M_3PO_4 can then proceed to react as per reaction R5, resulting in an overall liberation of 4.5/7 (64%) of the oxygen initially present in $M_4P_2O_7$. This is in better agreement with the experimental observations. However, further investigation is required to confirm this hypothesis.

Only a couple of studies covering the carbothermic reduction of Na- and K-metaphosphates are available in the literature. Kalmykov et al. [14] investigated the reaction between ultraphosphates ($M_2O/P_2O_5 < 1$) and activated birchwood charcoal or graphite at 1000, 1100, and 1250 °C. At the lower temperatures, vaporization of P_2O_5 and MPO_3 were suggested to be the main processes, whereas at higher temperatures reduction to elemental P also took place. However, the composition of the solid products did not increase much beyond a M_2O/P_2O_5 molar ratio of 1, suggesting that once the P_2O_5 fraction not associated with cations has reacted, the residual MPO_3 reacts to release M:P in a 1:1 ratio or is vaporizing congruently. Later, Shevchenko et al. [16] studied the reaction of the metaphosphates $NaPO_3$ and KPO_3 with activated birchwood charcoal, at the same temperatures. At 1000 °C, the M_2O/P_2O_5 molar ratio in the solid residue increased with time, suggesting that a reduction, causing release of P takes place [16]:

$$4MPO_3(l) + 5C(s) \rightarrow M_4P_2O_7(s) + \tfrac{1}{2}P_4(g) + 5CO(g) \quad (R9)$$
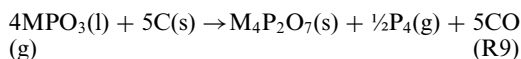
At 1250 °C, the M_2O/P_2O_5 molar ratio did not change, but the ratio of released CO/P was 2.5, which made the authors suggest that the following reaction takes place [16]:

$$MPO_3(l) + \tfrac{5}{2}C(s) \rightarrow \tfrac{1}{2}M_2O(g) + \tfrac{1}{4}P_4(g) + \tfrac{5}{2}CO(g) \quad (R10)$$
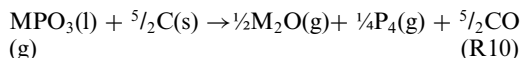
However, in the present work the CO/P ratio is around 3, indicating that the released alkali is not bound to oxygen, but rather leaving as M(g). This is reasonable considering the low stability of $M_2O(g)$ and the reducing conditions in the carbon bed. This would mean the reaction can be summarized as:

$$MPO_3(l) + 3C(s) \rightarrow M(g) + \tfrac{1}{4}P_4(g) + 3CO(g) \quad (R11)$$
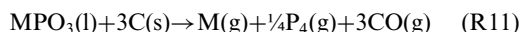
Whether a reaction such as R9 is first taking place, or reduction of MPO_3 takes place in one step as described by R11 cannot be concluded with the present data. Considering that both the $CO+CO_2$ and TGA data reveal the presence of one major peak, the latter seem likely. However, recently a similar experiment with $NaPO_3$ and the same carbon source as used in this work, but prepared with a significantly lower ratio of C/P (about 1/1) in the mixture, showed that mainly P was released [11].

Not all alkali and P seem to have left the samples at the end of the experiments, even though the reaction appears to have reached completion based on the low $CO+CO_2$ concentration in the off-gas. For both the Na- and the K-phosphates, the amount of alkali and P that remained in the sample is similar. The alkali/P molar ratio in the final sample was in the range 2.5–3.7 for the K-phosphates and 2.1–2.2 for the Na-phosphates. There are a few possible explanations for the residual alkali and P:

(1) Simultaneously with the reaction causing release of P, a parallel reaction might take place in which only CO is liberated and P forms alkali phosphide(s) that remain in the sample.
(2) Some of the released Na/K(g) and P(g) might react with the solid (or liquid) phosphates in the sample to form phosphite(s) and/or phosphide(s) that are more or less stable in the temperature range investigated.
(3) The small amount of Al (1 wt%) and Si (3 wt%) present in the sample residues (originating from the activated carbon) might capture some of the released alkali and P.

A test using different bed heights was performed (details in the SM), since the mass loss would be expected to vary with bed height in the case of (2) and (3). The bed height did not affect the mass loss, so formation of phosphides (1) may account for the residual alkali and P, rather than reactions between released species and phosphates (2) or Al and Si (3). K and Na phosphides decompose to yield gaseous alkali and P upon prolonged heating at the temperatures used in this work [30]. The TGA data show
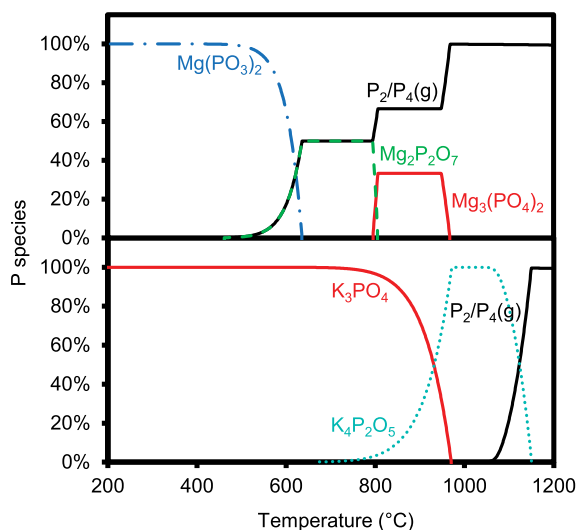
Fig 3. Distribution of P according to thermodynamic equilibrium calculations for $Mg(PO_3)_2$ (upper) and K_3PO_4 (lower). An input composition corresponding to 1.23 mol N_2, 181 mmol C, and 7.25 mmol P was used (the amount of oxygen and cation follows from the phosphate stoichiometry). The pressure was set to 1 atm. Species accounting for more than 1% of P are included.

that there is some mass loss also after the major peaks, possibly caused by alkali phosphide decomposition.

Thermodynamic equilibrium calculations

In Fig. 3, the association of phosphorus, based on the thermodynamic equilibrium calculations, is shown for $Mg(PO_3)_2$, here acting as an example for the alkaline earth phosphates. The result for K_3PO_4 is also shown since this work showed that an intermediate with the overall composition $K_4P_2O_5$ is present. The result for other phosphates are shown in the SM. The FactSage databases contain no thermodynamic data for possible species or melts of reduced Na- and K-phosphates, such as phosphites. This is not surprising as studies of such systems are lacking in the literature. To obtain a rough estimate for the thermodynamic properties of the proposed intermediate; $K_4P_2O_5$, the 'H, S, C_p Estimation Module' in the software HSC Chemistry 9 by Metso Outotec was used.

For the alkaline earth phosphates, the thermodynamic equilibrium calculations suggested that the reduction follow the process: meta → pyro → ortho → alkaline earth oxide. This fits well with the experimental observations in this work. However, the equilibrium calculations suggest the reductions to be favorable at lower temperatures compared to what was observed experimentally. This difference might be attributed to several factors; 1) mass transfer and/or reaction kinetics are limiting the processes, 2) the amount of carbon used in

the model might not represent the concentration locally at the interface between the carbon and phosphate particle, 3) the experimental system is a semi-batch process, and the amount of N_2 used in the modeling, as well as the partial pressure of released species, might not be representative.

The result for K_3PO_4 agrees well with the experimental observations in this work; first K_3PO_4 is reduced to the intermediate compound, and at higher temperatures a second reduction take place. However, the thermodynamic equilibrium calculations also predict the formation of $K_4P_2O_5$ for the phosphates KPO_3 and $K_4P_2O_7$, and at rather low temperatures, which may indicate that the estimated thermodynamic data is not representative for the intermediate. If $K_4P_2O_5$ is excluded from the thermodynamic calculations, the alkali phosphates are suggested to follow the reduction process: meta → pyro → ortho → alkali(g). The experimental results clearly indicated that is not the case. Hence, the behavior of the alkali phosphates cannot be satisfactorily described with the current thermodynamic data available.

It should be noted that no phosphorus oxides or alkali phosphates are predicted to be present in the gas phase.

All calculations showed that carbon was released only as CO, which agrees well with the experimental observations. Decreasing the C/P ratio from 25 to 3 did not affect the behavior of P in the calculations noticeably. Similarly, the O/P molar ratio could be increased from 3 to 4 (depending on the phosphate) up to around 25 while only affecting
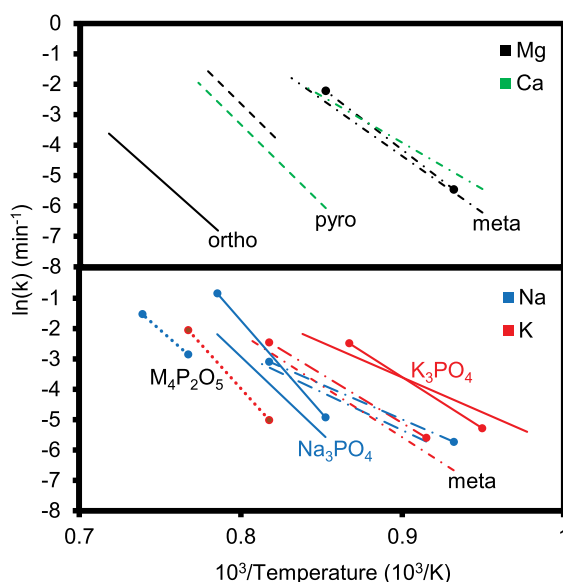
Fig 4. Arrhenius plot of the carbothermic reduction reactions R2-R4 for the alkaline earth phosphates (top), and R5, R6, and R11 for the alkali phosphates (bottom). Line-ends with and without filled circles indicate calculation based on TGA data and $CO+CO_2$ measurement respectively.

the P release by shifting it towards somewhat higher temperatures. These observations shows that, in case oxygen is available to convert all carbon to CO, which is not as powerful a reducing agent, less P will be released.

Kinetics

To allow for a comparison of the reactivity of the different phosphates, reaction rates were calculated using $CO+CO_2$ data from the tube reactor experiments and using TGA data. The results are shown in Fig. 4 (the experimental data, including the linear fits, are shown in the SM). A TGA run was performed using $Mg(PO_3)_2$ to verify that the calculated rates are similar for the two methods. The alkali pyrophosphates were not included because the specific reaction taking place is unclear. Due to the multiple small peaks in the $CO+CO_2$ profile for $Ca_3(PO_4)_2$, the fit was rather poor and the results therefore excluded. Generally, the calculation based on TGA data corresponds well with the value from the $CO+CO_2$ measurement. However, the result based on the $CO+CO_2$ measurement appears to be shifted to somewhat higher temperatures. The shift might be caused by a slower heating of the larger sample in the horizontal tube reactor compared to the small sample analyzed using TGA.

For the alkaline earth phosphates, the meta- and pyrophosphates are grouped closely together. The alkali metaphosphates are also grouped together,

but at somewhat higher temperatures compared to the alkaline earth metaphosphates. The reason is unclear. However, at the reaction temperature, KPO_3 and $NaPO_3$ are present in liquid form, presumably as polyphosphates; $(MPO_3)_n$. The depolymerization rate of these chains was previously suggested to affect the reaction rate at higher temperatures [16], but whether this is actually causing the difference compared to alkaline earth phosphates is not known.

The large reaction rate of K_3PO_4 compared to Na_3PO_4 is noteworthy and would require further investigation to be clarified.

Conclusions

Carbothermic reduction reactions of phosphates relevant for thermal conversion of biomass were studied. It can be concluded that the meta-, pyro-, and orthophosphates of Na, K, Mg, and Ca react with carbon at temperatures (>850 °C) that are relevant for biomass combustion, gasification and pyrolysis.

Alkaline earth phosphates undergo reduction in the stepwise process; meta → pyro → ortho → alkaline earth oxide. The alkali phosphates do not follow the same process. With a C/P ratio of 25/1, alkali metaphosphates appear to be reduced in a single step, whereas a stable intermediate is formed for alkali pyro- and orthophosphates. The results in this work indicate the intermediate for the K-

phosphates is a phosphite with the overall composition $K_4P_2O_5$. Currently available thermodynamic data cannot describe the reduction process particularly well. Apart from P, the carbothermic reduction of alkali phosphates also results in the release of alkali, which is important because it can cause operational problems in thermal conversion processes.

Kinetic data for the different phosphates are presented and can be used for qualitative comparison of their reactivity and for providing an estimation of the release rate.

Declaration of Competing Interest

The authors declare that they have no known competing financial interests or personal relationships that could have appeared to influence the work reported in this paper.

Acknowledgements

Supplementary materials

Supplementary material associated with this article can be found, in the online version, at doi:10.1016/j.proci.2022.07.087.

References

[1] H. Wu, M. Castro, P.A. Jensen, F.J. Frandsen, P. Glarborg, K. Dam-Johansen, M. Røkke, K. Lundtorp, Release and transformation of inorganic elements in combustion of a high-phosphorus fuel, Energy Fuels 25 (7) (2011) 2874–2886.

[2] G. Eriksson, H. Hedman, D. Boström, E. Pettersson, R. Backman, M. Öhman, Combustion characterization of rapeseed meal and possible combustion applications, Energy Fuels 23 (8) (2009) 3930–3939.

[3] K. Singh, L.M. Risse, K.C. Das, J. Worley, S. Thompson, Effect of fractionation and pyrolysis on fuel properties of poultry litter, J. Air Waste Manag. Assoc. 60 (7) (2010) 875–883.

[4] B.L. Turner, A.B. Leytem, Phosphorus compounds in sequential extracts of animal manures: chemical speciation and a novel fractionation procedure, Environ. Sci. Technol. 38 (22) (2004) 6101–6108.

[5] M. Öhman, A. Nordin, K. Lundholm, D. Boström, Ash transformations during combustion of Meat-, Bonemeal, and RDF in a (bench-scale) fluidized bed combustor, Energy Fuels 17 (2003) 1153–1159.

[6] A. Grimm, N. Skoglund, D. Boström, M. Öhman, Bed agglomeration characteristics in fluidized quartz bed combustion of phosphorus-rich biomass fuels, Energy Fuels 25 (3) (2011) 937–947.

[7] J. Beck, J. Brandenstein, S. Unterberger, K.R.G. Hein, Effects of sewage sludge and meat and bone meal co-combustion on SCR catalysts, Appl. Catal. B Environ. 49 (1) (2004) 15–25.

[8] A. Hedayati, R. Lindgren, N. Skoglund, C. Boman, N. Kienzl, M. Öhman, Ash transformation during single-pellet combustion of agricultural biomass with a focus on potassium and phosphorus, Energy Fuels 35 (2) (2021) 1449–1464.

[9] D.J. Lane, P.J. Van Eyk, P.J. Ashman, C.W. Kwong, R. De Nys, D.A. Roberts, A.J. Cole, D.M. Lewis, Release of Cl, S, P, K, and Na during thermal conversion of algal biomass, Energy Fuels 29 (4) (2015) 2542–2554.

[10] X. Chen, H. Wu, Transformation and release of phosphorus during rice bran pyrolysis: effect of reactor configurations under various conditions, Fuel 255 (2019) 1–7 115755.

[11] E.O. Lidman Olsson, P. Glarborg, H. Leion, K. Dam-Johansen, H. Wu, Release of P from pyrolysis, combustion, and gasification of biomass—a model compound study, Energy Fuels 35 (19) (2021) 15817–15830.

[12] S.I. Lopatin, Vaporization in phosphate systems, Russ. J. Gen. Chem. 67 (2) (1997) 193–211.

[13] A.D.F. Toy, Chapter 20. Phosphorus, in: Chem. Phosphorus, Pergamon Press, Oxford, New York, 1973, pp. 389–406. Toronto, Sydney, Paris, Braunschweig.

[14] S.I. Kalmykov, N.P. Shevchenko, Y.N. Dyankova, About the properties of ultraphosphates of alkali and alkaline earth metals. Message XV. Investigation of the reduction of ultraphosphates of sodium, potassium, magnesium with carbon (in Russian), Izv. Akad. Nauk Kazachskoj SSR. Ser. Chim. 1 (1985) 7–14.

[15] N.P. Shevchenko, N.M. Ulanova, V.P. Kozhevnikova, G.N. Zhuravlev, Reduction of amorphous ternary sodium-potassium-magnesium ultraphosphate by carbon, J. Appl. Chem. Ussr. 63 (1) (1990) 6–10.

[16] N.P. Shevchenko, N.M. Ulanova, Kinetics and mechanism of carbon redoing of $(MPO_3)_n$ sodium and potassium phosphates (in Russian), Zhurnal Neorg. Khimii. 34 (7) (1989) 1704–1709.

[17] G.W. Morey, The System H_2O-$NaPO_3$, J. Am. Chem. Soc. 75 (23) (1953) 5794–5797.

[18] T. Vlase, G. Vlase, N. Doca, Kinetics of thermal decomposition of alkaline phosphates, J. Therm. Anal. Calorim. 80 (1) (2005) 207–210.

[19] R.K. Osterheld, L.F. Audrieth, Polymerization and depolymerization phenomena in phosphate-metaphosphate systems at higher temperatures. Condensation reactions involving the potassium hydrogen orthophosphates, J. Phys. Chem. 56 (1) (1952) 38–42.

[20] M. Pyldme, K. Tynsuaadu, F. Paulik, J. Paulik, M. Arnold, Dehydrations of $Ca(H_2PO_4)_2 \cdot H_2O$ and $Mg(H_2PO_4)_2 \cdot 2H_2O$ and their reactions with KCl, examined with simultaneous TG, DTG, DTA and EGA, J. Therm. Anal. 17 (2) (1979) 479–488.

[21] C.W. Bale, E. Bélisle, P. Chartrand, S.A. Decterov, G. Eriksson, A.E. Gheribi, K. Hack, I.H. Jung, Y.B. Kang, J. Melançon, A.D. Pelton, S. Petersen, C. Robelin, J. Sangster, P. Spencer, M.A. Van Ende, FactSage thermochemical software and databases,

2010-2016, Calphad Comput, Coupl. Phase Diagrams Thermochem 54 (2016) 35–53.

[22] W. Xie, S. Wei, P. Hudon, I.H. Jung, Z. Qiao, Z. Cao, Critical evaluation and thermodynamic assessment of the R_2O–P_2O_5 (R = Li, Na and K) systems, Calphad Comput. Coupl. Phase Diagrams Thermochem. 68 (2020).

[23] K.I. Yamamoto, A. Kato, T. Seiyama, Reduction of calcium phosphates with carbon (in Japanese), J. Soc. Chem. Ind. Japan. 71 (3) (1968) 367–372.

[24] P. Hudon, I.H. Jung, Critical evaluation and thermodynamic optimization of the CaO-P_2O_5 system, Metall. Mater. Trans. B. 46 (1) (2015) 494–522.

[25] D.I. Kriklivyi, Mechanism of reduction of tricalcium Orhophosphate, J. Appl. Chem. USSR. 57 (11) (1984) 2218–2225.

[26] Z. Gontarz, W. Wišniewski, Mechanism of the thermal decomposition of hydrophosphites of lithium, sodium and potassium, J. Therm. Anal. 38 (9) (1992) 2123–2128.

[27] D. Zobel, N. Ba, Studies on phosphite pyrolysis; reactions when heating Na_2HPO_3 in the absence of oxygen (in German), Zeitschrift Für Chemie 9 (347) (1969) 389–390.

[28] J.-.P. Ebel, N. Busch, G. Hertzog, Study of the thermal decomposition of sodium phosphites (in French), Bull. Soc. Chim. Fr. (1958) 203–207.

[29] D. Grant, D.S. Payne, S. Skledar, The pyrolysis of inorganic phosphites, J. Inorg. Nucl. Chem. 26 (12) (1964) 2103–2111.

[30] R.P. Santandrea, C. Mensing, H.G. Von Schnering, The sublimation and thermodynamic properties of the alkali metal phosphides Na_3P_7(s), K_3P_7(s), Rb_3P_7(s) and Cs_3P_7(s), Thermochim. Acta. 98 (1986) 301–311.